nated authigenic clay minerals in a substantial proportion of highly weathered continental debris and have important implications for global controls of elemental cycling.

REFERENCES AND NOTES

1. F. T. Mackenzie and R. M. Garrels, *Am. J. Sci.* **264**, 507 (1966).
2. J. M. Edmond *et al.*, *Earth Planet. Sci. Lett.* **46**, 1 (1979).
3. R. Wollast and F. T. Mackenzie, in *Silicon Geochemistry and Biogeochemistry*, S. R. Aston, Ed. (Academic Press, San Diego, CA, 1983), pp. 39–76; F. T. Mackenzie, in *Encyclopedia of Earth System Science*, W. A. Nierenberg, Ed. (Academic Press, San Diego, CA, 1992), pp. 431–445.
4. G. S. Odin and P. D. Fullagar, in *Green Marine Clays*, G. S. Odin, Ed. (Elsevier, Netherlands, 1988), pp. 295–332.
5. G. M. McMurthy and H.-W. Yeh, *Chem. Geol.* **32**, 189 (1981); T. G. Cole, *Geochim. Cosmochim. Acta* **49**, 221 (1985).
6. J. E. Mackin and R. C. Aller, *Cont. Shelf Res.* **6**, 245 (1986).
7. ______, *Geochim. Cosmochim. Acta* **48**, 281 (1984).
8. P. D. Rude and R. C. Aller, *Cont. Shelf Res.* **14**, 883 (1994).
9. B. L. Ristvet, thesis, Northwestern University, Evanston, IL (1978); F. T. Mackenzie, B. L. Ristvet, D. C. Thorstenson, A. Lerman, R. H. Leeper, in *River Inputs to the Ocean*, J. M. Martin, J. D. Burton, D. Eisma, Eds. (United Nations Environment Programme– United Nations Educational, Scientific, and Cultural Organization, Geneva, Switzerland, 1981), pp. 152–187.
10. P. D. Rude and R. C. Aller, *J. Sediment. Petrol.* **59**, 704 (1989).
11. This project was part of A Multidisciplinary Amazon Sediment Study (AMASEDS) [see C. A. Nittrouer, D. J. DeMaster, Á. G. Figuereido, J. M. Rine, *Oceanography* **4**, 3 (1991)].
12. J. D. Milliman and J. P. M. Syvitski, *J. Geol.* **100**, 525 (1992).
13. R. J. Gibbs, *Geol. Soc. Am. Bull.* **78**, 1203 (1967).
14. K. O. Konhauser, W. S. Fyfe, B. I. Kroeberg, *Chem. Geol.* **111**, 155 (1994).
15. R. C. Aller, J. E. Mackin, R. T. Cox Jr., *Cont. Shelf Res.* **6**, 263 (1986); R. C. Aller, N. E. Blair, Q. Xia, P. D. Rude, *ibid.*, in press.
16. Substrate (i) was Ward's kaolinite standard no. 9, collected from Mesa Alta, NM. Substrate (ii) was quartz sand, grain size 200 to 400 μm. Substrate (iii) was quartz sand grains coated with a FeOOH-gel made from $FeCl_3$ and NaOH at a pH of 5. The resulting coating was x-ray amorphous, and the probable compound was FeOOH. For substrate (iv), the beads were made out of glass composed mostly of Si and containing some Ca, Na, and Mg. Size range was 20 to 60 μm.
17. Submicron crystallites composed of Si, Al, K, Fe, and Mg and having a curved morphology were ubiquitous under the TEM.
18. We did not analyze lattice spacings (d) larger than 10.2 Å. Because of the small amount of material available for x-ray diffraction analysis, we used a capillary tube sample holder and a synchrotron radiation source at Brookhaven National Laboratory. The wavelength used in conjuction with the geometry of the sample holder–detector setup did not allow data acquisition at low angles. Powder diffraction patterns also showed the presence of amorphous material.
19. It is possible that the presence of any K-poor phase might have contaminated the analyses of the K-Fe–rich phase. We also cannot exclude the possibility of mixed layering. In addition, it is difficult to assess the contribution from the amorphous material present in the precipitates. More than 90% of the analyses were dominated by the inferred K-Fe phase.
20. The pH of the sediments after the termination of the experiments was within the range of the in situ values measured during collection (7.2 to 7.4). Analysis of the pore waters after the termination of the experiments showed that Mg, Ca, Si, Fe, and total CO_2 concentrations were in the range measured in shelf pore waters.
21. G. S. Odin and A. Matter, *Sedimentology* **28**, 611 (1981).
22. Low-temperature (3° to 22°C) formation of clay minerals has also been observed under a variety of artificial laboratory conditions [H. Harder, *Chem. Geol.* **18**, 169 (1976); *Clays Clay Miner.* **26**, 65 (1978); *ibid.* **28**, 217 (1980)].
23. This value is approximately 25% lower than previously estimated in (7), based on a combination of pore water gradient data and reaction rate measurements.
24. E. K. Berner and R. A. Berner, *The Global Water Cycle: Geochemistry and Environment* (Prentice-Hall, Englewood Cliffs, NJ, 1987), chap. 8.
25. A. J. Spivack and H. Staudigel, *Chem. Geol.* **115**, 239 (1994).
26. A. C. Aplin, in *Geochemistry of Clay-Pore Fluid Interactions*, D. A. C. Manning, P. L. Hall, C. R. Hughes, Eds. (Chapman and Hall, London, 1993), pp. 81–106; J. E. Mackin and R. C. Aller, *Crit. Rev. Aquat. Sci.* **1**, 537 (1989).
27. D. J. DeMaster, G. B. Knapp, C. A. Nittrouer, *Geochim. Cosmochim. Acta* **47**, 1713 (1983); D. J. DeMaster, W. O. Smith Jr., D. M. Nelson, J. Y. Aller, *Cont. Shelf Res.*, in press.
28. P. Tréguer *et al.*, *Science* **268**, 375 (1995).
29. R. C. Morris and A. B. Fletcher, *Nature* **330**, 558 (1987); L. M. Mayer, J. Jorgensen, D. Schnitker, *Mar. Geol.* **99**, 263 (1991).

30. We thank R. Reeder for obtaining the TEM data, M. Kunz and J. Parise for obtaining the synchrotron powder diffraction data, and G. Symmes for assisting with the microprobe analyses. P. Rude, M. Green, and J. Mackin helped with the probe construction and experimental setup. P. Bartholomew assisted with SEM-EDS analyses. The participants of AMASEDS assisted in all aspects of the field work. Financial support was provided by NSF (R.C.A). A fellowship from the State Scholarship Foundation of Greece to P.M. is acknowledged.

27 April 1995; accepted 31 July 1995

Limits to Relief

Kevin M. Schmidt* and David R. Montgomery

Comparison of slope profiles in areas exhibiting widespread bedrock landsliding with the use of a model for the maximum size of stable hillslopes established that mountain-scale material strength can limit topographic relief. Conventional laboratory values for intact rock greatly exceeded integrative rock strength properties that were back-calculated from the upper limit to hillslope relief and gradient in the northern Cascade Range and Santa Cruz Mountains. Back-calculated strength values, however, were indistinguishable from those obtained through field and conventional laboratory measurements on the weakest members of each rock formation, as well as on glacial sediments along the Cascade front. These results contrast with the conventional assumption that relief is incision-limited and indicate that the relief of mountain ranges can reflect landscape-scale material strength, as well as the interaction of tectonic and climatic processes.

Relief is a fundamental landscape attribute that is widely recognized as reflecting the interplay of uplift and erosion (*1*). The role of material properties in relief development, however, is poorly understood. The conventional view that the relief of natural landscapes is incision-limited (*2*) reflects the observation that hillslope stability analyses using intact rock strengths predict the stability of cliffs kilometers in height (*3*). However, rock mass strength decreases with increasing spatial scale, because of the influence of spatially distributed discontinuities (*4*), and it has been unclear whether mountain-scale rock strength might be low enough to limit relief in bedrock landscapes (*1*). Through a regional field test of a slope stability model, we demonstrate here that mountain-scale material strength can limit relief development in bedrock landscapes.

A model for bedrock landsliding provides a framework for prediction of the maximum size of stable hillslopes or mountain fronts and thereby for the evaluation of the influence of material properties on relief development (*5*). As hillslope relief (H) increases, topographically induced gravitational shear stress across potential failure surfaces increases until it exceeds material strength and landsliding ensues. Culmann's two-dimensional, limit-equilibrium, slope stability model (*6*), which has been widely applied to unconsolidated deposits (*7*), predicts a bounding relation between hillslope gradient (β) and relief such that the maximum hillslope height (H_c) is given by

$$H_c = \frac{4c}{\gamma} \frac{\sin\beta \cos\phi}{[1 - \cos(\beta - \phi)]} \qquad (1)$$

where c is cohesion, γ is unit weight, and ϕ is the internal friction angle. Hoek and Bray (*8*) modified Eq. 1 to incorporate pore water pressure, and Schmidt (*9*) integrated seismic accelerations. Assigning a representative γ, we used Eq. 1 to calculate landscape-scale c and ϕ from the upper limit to the range of β and H within a landscape. The actual material properties of incision-limited landscapes will exceed back-calculated values of c and ϕ, which indicates that bedrock strength could support deeper val-

Department of Geological Sciences, University of Washington, Seattle, WA 98195, USA.

*To whom correspondence should be addressed.

leys. In strength-limited landscapes, however, back-calculated and actual material properties should be equivalent, such that observed combinations of β and H define a limit to topographic development (LTD) beyond which incision of valley bottoms will induce bedrock landsliding that lowers peak elevations.

We analyzed hillslopes composed of the Eocene Chuckanut Formation and the overlying Quaternary glacial sediments located in the western Cascade Range of Washington state, as well as a sedimentary sequence in the Santa Cruz Mountains of central California. Widespread deep-seated landsliding in each study area implies that the observed relief approaches the LTD. We used aerial photograph analyses and earlier mapping (*10*) to identify deep-seated landslides; field surveys and measurements from topographic maps defined β and H. For each geologic sequence, we made a suite of transects from ridgetop to valley bottom to establish the local relief and maximum gradient (*11*). We fit the LTD for each unit to the upper envelope of β and H and used these back-calculated strength properties to predict the LTD both under saturated conditions and for horizontal seismic accelerations of 0.6*g*.

In Washington state, we mapped from aerial photographs over 585 km^2 along the United States–Canada border, an area encompassing the low-relief San Juan Islands as well as the higher relief landscape near the western flank of Mount Baker. We identified 34 mountain-front–scale bedrock landslides within the Chuckanut Formation (*9*), a sequence of alternating intervals of coarse- and fine-grained alluvial strata (*12*). Tertiary deformation compressed the sequence into broad northwest-plunging folds and high-angle faults. We differentiated hillslopes into dip and anti-dip slopes because large-scale structural anisotropy provides a strong control on hillslope strength (*13*). A plot of β versus H for measured transects revealed an arcuate upper bound characterizing the maximum observed topographic expression (Fig. 1). The LTD defined by the upper limit of the observed data for anti-dip slopes yielded $\phi = 21°$ and c = 150 kPa (Fig. 1A), whereas the threshold for dip slopes defined lower strength values of $\phi = 17°$ and c = 120 kPa (Fig. 1B). In situ measurements with a variably loaded sheargraph (*14*) on weak siltstone interbeds produced comparable strength values of $\phi = 27°$ and c = 26 kPa (*9*).

Quaternary glacial sediments in northwestern Washington on the west flank of the Cascade Range comprise a varied sequence of stiff, laminated lacustrine clay overlain by outwash sand and gravel and subsequently capped by boulder till. We treated the sequence as a single material unit in order to characterize the regional topographic development within glacio-fluvial deposits occupying valley floors. Within this unit, landslide thicknesses typically constitute a substantial proportion of relief, and the movement of landslide toes away from the hillslope face decreases post-failure hillslope gradients. Where possible, we reconstructed pre-landslide geometries from adjacent stable hillslopes. The LTD defined by β and H values from 178 field-surveyed transects along four channels (Middle Fork of the Nooksack River, Clearwater Creek, Rocky Creek, and Boulder River) yielded back-calculated strength values of $\phi = 29°$ and c = 20 kPa (Fig. 1C). Mean in situ properties measured with a variably loaded sheargraph in sandy silt outwash deposits were $\phi = 36° \pm 11°$ and $c = 12 \pm 9$ kPa (*9*).

The Santa Cruz Mountains of central California experienced widespread landsliding during the (magnitude) 7.1 Loma Prieta earthquake in 1989 (*15*). Landslides were concentrated in the high-relief, moderate-gradient, mountainous epicentral region as well as along the relatively low relief, high-gradient coastal cliffs along Monterey Bay. We measured hillslope attributes from topographic maps for 82 coseismic landslides in a sequence of lithologically similar marine sedimentary rocks from the Eocene to the Pliocene (*16*). The resulting LTD for the dry state yielded strength values of ϕ = 20° and c = 60 kPa. For comparison, triaxial and direct shear tests on the highly fractured, variably weathered, interbedded, and sheared sandstone, siltstone, and shale identified in slip surfaces of deep-seated landslides provided estimates of actual material strength controlling landslide displacement. Averaging values reported for fractured shale (*17*), the most common slide-plane material identified in drill cores, produced mean values of $\phi = 20° \pm 6°$ and

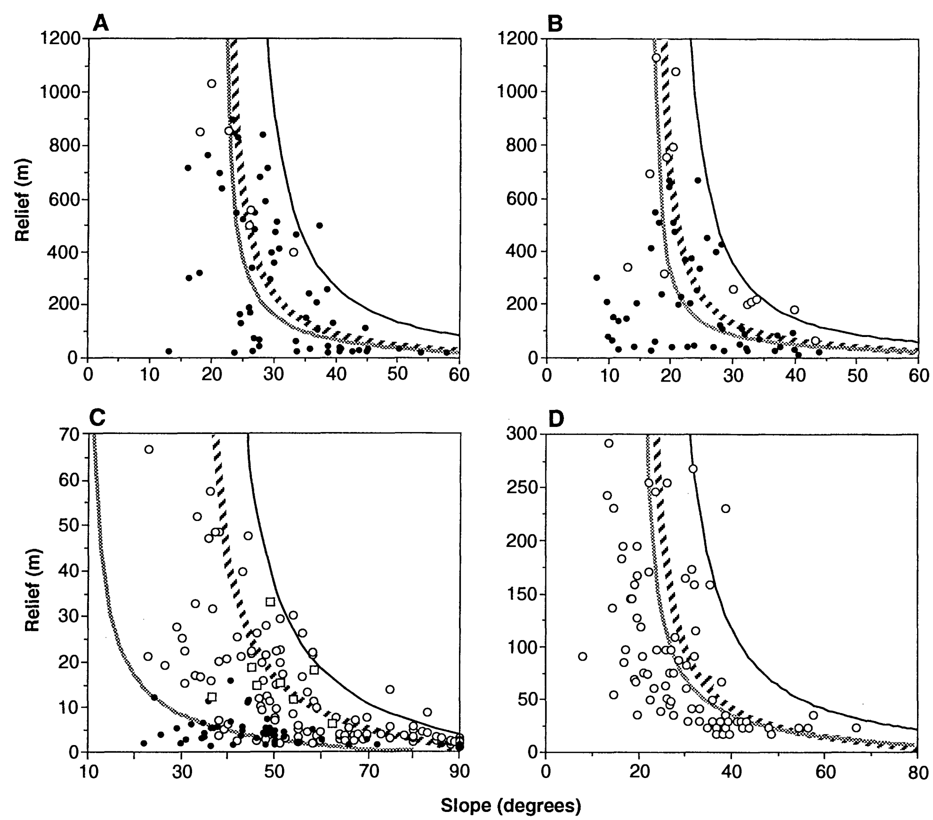

Fig. 1. Gradient versus relief for stable hillslopes (●), for landslide sites (○), and for reconstructed prefailure geometry of landslide sites (□) composed of three geologic units: the Eocene Chuckanut Formation, Quaternary glacio-fluvial sediments, and Eocene-to-Pliocene sediments of the Santa Cruz Mountains. Three LTD thresholds are depicted for each unit: dry conditions (solid black curve), saturated conditions (thick hatched curve), and horizontal seismic accelerations of 0.6*g* (gray curve). The LTD for the dry case was fit to the upper envelope of observations. Back-calculated strength properties from the dry case were used to investigate the influence of transient fluctuations caused by extreme pore pressures and seismic accelerations (*8*, *9*) that temporarily suppress the LTD. (**A**) Anti-dip slope transects for the Chuckanut Formation measured from 1 : 24,000-scale topographic maps. Back-calculated strength properties are ϕ = 21° and c = 150 kPa. (**B**) Dip slope transects for the Chuckanut Formation measured from 1 : 24,000-scale topographic maps. Back-calculated strength properties are ϕ = 17° and c = 120 kPa. (**C**) Transects for Quaternary glacio-fluvial deposits surveyed with a hand level, a stadia rod, and tape. Back-calculated strength properties are ϕ = 29° and c = 20 kPa. Extreme suppression of seismic LTD results from the assumption of coseismic failure plane generation. (**D**) Landslide sites for marine sedimentary units of the Santa Cruz Mountains. Back-calculated strength properties are ϕ = 20° and c = 60 kPa.

$c = 69 \pm 32$ kPa. Similarly, mean strength properties for all lithologies (shale, siltstone, sandstone, and clay) were $\phi = 30° \pm 14°$ and $c = 69 \pm 32$ kPa (*17*).

Large earthquakes commonly trigger landslides over areas of 10^5 to 10^6 km^2 (*18*). To predict the degree of earthquake-induced LTD suppression, we modeled seismic accelerations as horizontal body forces oriented out of the hillslope face (9). The relative timing of failure plane generation, either aseismic or coseismic, is crucial to the degree of LTD suppression. We suspect that most landslides within unconsolidated glacial sediments form coseismically, with slip surface inclinations dictated by the strong motion magnitude. In contrast, failure planes within the Chuckanut Formation and formations of the Santa Cruz Mountains are considered to form progressively. Suppression of the LTD under horizontal accelerations of 0.6*g* exceeds that for complete saturation (Fig. 1). Glacial sediments exhibit the highest degree of LTD suppression (Fig. 1C) because failure surfaces are considered to form coseismically (9). Hence, the model implies that incised glacial deposits are prone to extensive landsliding during earthquakes. The combination of earthquake-induced landslides with measured seismic accelerations in the epicentral region of the 1989 Loma Prieta earthquake provides an opportunity to test model predictions. Four strong-motion instruments located throughout the epicentral region recorded free-field peak horizontal accelerations from 0.47 to 0.64*g* during the main shock of 17 October 1989 (*19*). Although LTD suppression under horizontal accelerations of 0.6*g* roughly agrees with the landslide distribution (Fig. 1D), the presence of landslides below the seismically suppressed regional LTD may reflect the long-term impact of repeated seismic disturbance, which loosens rock masses and reduces hillslope shear resistance, in addition to spatially variable rock properties and saturation frequency.

The close agreement between strength parameters back-calculated from the LTD method and those derived from field and laboratory tests of the weakest members in a rock mass indicates that large-scale rock strength may control the regional LTD. Values for material properties back-calculated from the LTD approach are lower than those determined by traditional laboratory analyses on intact samples of coherent material but agree with values reported for unconsolidated materials and for the weakest members of a rock mass (Table 1). Although high *c* values are common for intact rock, material discontinuities can dramatically reduce bulk cohesion. Properties determined from the LTD for the Santa Cruz Mountains are equivalent to triaxial and direct shear tests (*17*) on fractured shale beds within landslide slip surfaces (Table 1). Additionally, in situ sheargraph tests on glacial sediments yield values comparable to those given by the LTD approach. This agreement between disparate methods supports the fundamental approach of the LTD model.

Although representation of mountain-scale material properties is essential to the prediction of landscape development and landslide hazards, a stark dichotomy exists between the spatial and temporal scales of conventional laboratory analyses and their application to geologic problems. Small samples of intact rock used in laboratory tests yield strength parameters that are stronger than those of the entire rock mass, because the shear surface is restricted to a narrow sampling of the available discontinuities. Furthermore, apparent rock strength depends on applied stress rate (*20*). Typical strength tests thus overestimate material strength, because the duration of applied stress is orders of magnitude shorter and the failure plane is orders of magnitude smaller in surface area than are those for natural hillslopes.

No theory exists for independently predicting the specific LTD for a mountain range, but regions with considerable relief and steep gradients, such as active tectonic areas with rapid rock uplift, typically display widespread bedrock landsliding (*21*). In these areas, rock mass strength rather than valley incision rates may limit relief development. This control on landscape evolution is crucial to understanding the relation between climate, valley incision, and the uplift of mountain peaks. The attribution of late Cenozoic uplift of mountain ranges to increased valley incision and subsequent isostatic compensation (*22*), for example, assumes that relief can be increased by the incision of deep valleys. The similarity between back-calculated, large-scale, rock mass strength properties and engineering tests on the weakest members of rock formations implies that bedrock landsliding could inhibit valley incision, especially in mountain ranges composed of highly deformed or weak rock. Although it is recognized that relief reflects the interaction of valley incision and rock uplift, our results indicate that landscape-scale rock strength may also limit the relief of mountain ranges.

Table 1. Strength properties back-calculated from topographic expression (LTD), measured in situ with a sheargraph (*9, 14*) and derived from laboratory tests (*8, 17*).

Material	Friction angle (ϕ) (degrees)	Cohesion (*c*) (kPa)	Source
Chuckanut Formation (anti-dip slope)	21	150	LTD (this study)
Chuckanut Formation (dip slope)	17	120	LTD (this study)
Chuckanut Formation (siltstone)	27	26	In situ sheargraph measurement (*9*)
Hard sedimentary rock (sandstone)	35 to 45	10,000 to 30,000	Laboratory experiments (*8*)
Soft sedimentary rock (shale or coal)	25 to 35	1,000 to 20,000	Laboratory experiments (*8*)
Santa Cruz Mountains	20	60	LTD (this study)
Santa Cruz Mountains (shale)	20 ± 6	69 ± 32	Laboratory experiments (*17*)
Santa Cruz Mountains (shale, siltstone, sandstone, and clay)	30 ± 14	69 ± 32	Laboratory experiments (*17*)
Glacial sediments	29	20	LTD (this study)
Glacial sediments (sandy outwash)	36 ± 11	12 ± 9	In situ sheargraph measurement (*9*)

REFERENCES AND NOTES

1. F. Ahnert, *Am. J. Sci.* **268**, 243 (1970); *ibid.* **284**, 1035 (1984). Ahnert recognized that the ratio of mountain range relief to the base length is nearly a constant value, and thus that broad mountain ranges support a great deal of relief.
2. The ability of channel networks to incise valley bottoms controls the relief of incision-limited landscapes, whereas rock mass strength regulates the relief of strength-limited landscapes by determining the maximum size of stable hillslopes.
3. K. Terzaghi [*Géotech.* **12**, 251 (1962)] describes the critical height of a vertical slope in unweathered, mechanically intact rock as $H_c = q_u/\gamma$, where H_c is the maximum stable relief, q_u is the unconfined compressive strength, and γ is the unit weight. The unconfined compressive strength, as a stress, is simply the weight of rock per unit area of the base ($H_c\gamma$). Average laboratory-derived properties for intact sandstone, q_u = 100 MN/m^2 and γ = 20 kN/m^3, predict an unrealistic vertical slope height of 5 km.
4. Z. T. Bieniawski and W. L. Van Heerden, *Int. J. Rock Mech. Min. Sci.* **12**, 101 (1975); H. Jahns, in *Proceedings of the 1st Congress of the International Society of Rock Mechanics*, Lisbon, Portugal, 25 September to 1 October 1966 (Laboratório Nacional de Engenharia Civil, Lisbon, Portugal, 1966), vol. 1, pp. 477–482; E. Richter, *Bergakademie* **20**, 721 (1968); H. R. Pratt, A. D. Black, W. D. Brown, W. F. Brace, *Int. J. Rock Mech. Min. Sci.* **9**, 513 (1972).
5. Examples of deep-seated bedrock landslides limiting local relief include the recent summit collapse and lowering of New Zealand's tallest peak, Mount Cook [G. T. Hancox, T. J. Chinn, M. J. McSaveney, *File Reference H36/942* (New Zealand Department of Scientific and Industrial Research, Lower Hutt, New Zealand, 1991)] and the historical landslides at Hope, British Columbia, Canada [W. H. Matthews and K. C. McTaggart, in *Rock-*

slides and Avalanches, 1, B. Voight, Ed. (Elsevier, Amsterdam, 1978), pp. 259–275], and Gros Ventre, WY (B. Voight, *ibid.*, pp. 113–166).
6. C. Culmann, *Die Graphische Statik* (Meyer and Zeller, Zürich, Switzerland, 1875).
7. Studies determining material properties from topographic limits have been applied to clay strata in England [W. Skempton, *Proc. Yorks. Geol. Soc.* **29**, 33 (1953)], to friable loess deposits in Iowa [R. A. Lohnes and R. L. Handy, *J. Geol.* **76**, 247 (1968)], to coastal bluffs composed of glacial deposits [W. S. McGreal, *Z. Geomorphol. Suppl.* **23**, 76 (1979)], and to loess-derived alluvium in Tennessee [A. Simon, in *Applied Quaternary Research*, E. F. J. DeMulder and B. P. Hageman, Eds. (Balkema, Rotterdam, Netherlands, 1989), pp. 129–146; A. Simon and C. R. Hupp, *U.S. Geol. Surv. Open-File Rep. 91-502* (1992)].
8. E. Hoek and J. W. Bray, *Rock Slope Engineering* (Institute of Mining and Metallurgy, London, 1977).
9. K. M. Schmidt, thesis, University of Washington, Seattle (1994).
10. A. J. Fiksdal and M. J. Brunengo, *Forest Slope Stability Project Phase II* (Washington State Department of Ecology, Olympia, WA, 1981).
11. M. J. Selby [*Z. Geomorphol. Suppl.* **24**, 31 (1980)] related finer scale variations in the gradient of bedrock hillslopes to outcrop-scale rock mass strength.
12. S. Y. Johnson, thesis, University of Washington, Seattle (1982); *Can. J. Earth Sci.* **21**, 92 (1984).
13. K. M. Schmidt and D. R. Montgomery, in preparation.
14. A variably loaded sheargraph is a portable instrument used to determine in situ strength properties of earth materials. A cup is seated with a given normal force, and the material is sheared until failure occurs. By variation of the normal force and thus of the associated shear force, a suite of values is produced that, in conjunction with Mohr-Coulomb failure theory, determines friction angle and cohesion.
15. G. Plafker and J. P. Galloway, Eds., *U.S. Geol. Surv. Circ. 1045* (1989); T. E. Spittler, E. L. Harp, D. K. Keefer, R. C. Wilson, R. H. Sydnor, in *The Loma Prieta (Santa Cruz Mountains), California, Earthquake of 17 October 1989*, S. R. McNutt and R. H. Sydnor, Eds. (Department of Conservation, Division of Mines and Geology, Sacramento, CA, 1990), pp. 59–66; T. E. Spittler and E. L. Harp, *U.S. Geol. Surv. Open-File Rep. 90-688* (1990).
16. Landslides triggered by the 1989 Loma Prieta earthquake were mapped in seven geologic units: Butano Sandstone, San Lorenzo Formation, Santa Cruz Mudstone, Vaqueros Sandstone, Santa Margarita Sandstone, Monterey Formation, and Purisima Formation. As the combined thickness of the above listed sequence exceeds the local relief, the sequence was considered as a single material unit in order to examine regional topographic development.
17. Strength properties reported by D. K. Keefer [*U.S. Geol. Surv. Open-File Rep. 91-618* (1991)] were determined from drill core samples (<7.3 cm in diameter) of landslide failure planes.
18. D. K. Keefer, *Geol. Soc. Am. Bull.* **95**, 406 (1984); R. C. Wilson and D. K. Keefer, Eds., *U.S. Geol. Surv. Prof. Pap. 1360* (1985).
19. D. M. Boore, L. Seekins, W. B. Joyner, *Seism. Res. Lett.* **60**, 151 (1989); A. F. Shakal, M. J. DeLisle, M. S. Reichle, R. B. Darragh, in *The Loma Prieta (Santa Cruz Mountains), California, Earthquake of 17 October 1989*, S. R. McNutt and R. H. Sydnor, Eds. (Department of Conservation, Division of Mines and Geology, Sacramento, CA, 1990), pp. 29–46; R. H. Sydnor, G. B. Griggs, G. E. Weber, R. J. McCarthy, N. Plant, *ibid.*, pp. 67–82.
20. R. H. Schmidtke and E. Z. Lajtai, *Int. J. Rock Mech. Min. Sci.* **22**, 461 (1985); E. Z. Lajtai and R. H. Schmidtke, *Rock Mech. Rock Eng.* **19**, 11 (1986).
21. Ascertaining that bedrock landsliding indeed limits relief over geologic time is complicated because only a portion of a landscape displays active landsliding at any one time, and older deposits are often poorly preserved or removed by fluvial or glacial transport. Thus, it may prove difficult to test whether rates of material removal by bedrock landsliding are commensurate with regional erosion rates.
22. P. England and P. Molnar, *Geology* **18**, 1173 (1990); P. Molnar and P. England, *Nature* **346**, 29 (1990).
23. Supported by the Washington State Timber/Fish/Wildlife Agreement (grants FY92-010 and FY94-004) and by gifts from the Washington Forest Protection Association and the Weyerhaeuser Company. Special thanks are extended to T. Dunne; to field assistants Y. Merrand, V. Langenheim, and J. Stock; and to two anonymous reviewers.

6 June 1995; accepted 25 August 1995

Megascopic Multicellular Organisms from the 1700-Million-Year-Old Tuanshanzi Formation in the Jixian Area, North China

Zhu Shixing and Chen Huineng

Hundreds of specimens of megascopic carbonaceous fossils shaped like leaves have been found at the ~1700-million-year-old Tuanshanzi Formation of the uppermost Paleoproterozoic Changcheng Group (1600 to 1850 million years old) in the Jixian area, north China. These leaflike fossils mostly resemble the *Longfengshania*; each consists of a blade (with spoonlike, lanceolate, or ribbonlike shapes) with a single stipe, a holdfast, or both. On the basis of their megascopic dimensions, preliminary differentiation of organs or tissues, and possible remains of multicellular structures, they are benthic, multicellular algal fossils similar to the longfengshanids. These fossils indicate that multicellular organisms originated at least 1700 million years ago.

The emergence of multicellular organisms (metaphytes and metazoans) is an important event in the evolutionary history of Precambrian life since the emergence of unicellular eukaryotes. The oldest remains of multicellular organisms are therefore one of the keys to the early evolution of life on Earth. A few megascopic carbonaceous films of *Tyrasotaenia* from the 1700-million-year-old Tuanshanzi Formation of the Changcheng Group in the Jixian area, north China, have been reported (*1*) but have not been widely accepted as multicellular organisms (*2*, *3*).

In addition to a few samples of ribbonlike and sausagelike megafossils resembling the vendotaenids and tawuids, respectively, we have recently found more than 300 specimens of megascopic carbonaceous fossils shaped like leaves from the locality and horizon close to that described in (*1*). These leaflike megafossils have obvious characteristics of multicellular algae. The megascopic carbonaceous remains were found near Tuanshanzi Village and its adjacent area (40°10′N, 117°27′E), about 20 km northeast of Jixian Town (Fig. 1). The best-preserved specimens came from the lower part (first member) of the Tuanshanzi Formation, ~44 to 47 m above its base (Fig. 2). The Tuanshanzi Formation belongs to the Paleoproterozoic Changcheng Group. The group includes the Changzhougou (conglomerate, sandstone), Chuanlinggou (silty and illitic shale), Tuanshanzi (muddy and silty dolomicrite), and Dahongyu (sandstone, volcanic rocks, cherty dolomicrite) formations in ascending order, and has a total thickness of

Tianjin Institute of Geology and Mineral Resources, Chinese Academy of Geological Sciences, 4 Eighth Road, Dazhigu, Tianjin 300170, People's Republic of China.

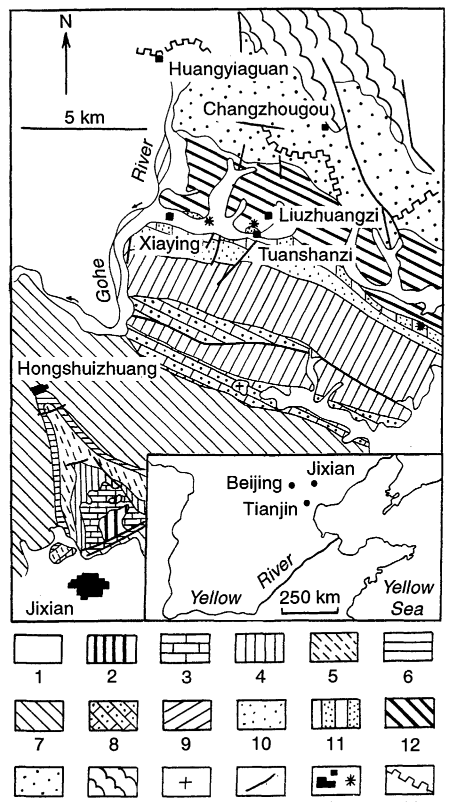

Fig. 1. Location map and geological map of the Jixian area (1, Quaternary; 2, Cambrian; 3, Changlongshan-Jing'eryu Formation; 4, Xiamaling Formation; 5, Tieling Formation; 6, Hongshuizhuang Formation; 7, Wumishan Formation; 8, Yangzhuang Formation; 9, Gaoyuzhuang Formation; 10, Dahongyu Formation; 11, Tuanshanzi Formation; 12, Chuanlinggou Formation; 13, Changzhougou Formation; 14, Archean; 15, Mesozoic granite; 16, fault; 17, town, village, and new fossil occurrences; and 18, Great Wall).